NUCL SCI TECH (2021) 32:59
https://doi.org/10.1007/s41365-021-00900-3

Populating ^{229m}Th via two-photon electronic bridge mechanism

Neng-Qiang Cai[1,2] · Guo-Qiang Zhang[2,3] · Chang-Bo Fu[4] · Yu-Gang Ma[1,2,4]

Received: 24 March 2021 / Revised: 21 April 2021 / Accepted: 7 May 2021 / Published online: 12 June 2021

Abstract The isomer ^{229m}Th is the most promising candidate for clocks based on the nuclear transition because it has the lowest excitation energy of only 8.10 ± 0.17 eV. Various experiments and theories have focused on methods of triggering the transition between the ground state and isomeric state, among which the electronic bridge (EB) is one of the most efficient. In this paper, we propose a new electronic bridge mechanism via two-photon excitation based on quantum optics for a two-level nuclear quantum system. The long-lived $7s_{1/2}$ electronic shell state of $^{229m}Th^{3+}$, with a lifetime of approximately 0.6 s, is chosen as the initial state and the atomic shells (7s–10s) could be achieved as virtual states in a two-photon process. When the virtual states return to the initial state $7s_{1/2}$, there is a chance of triggering the nucleus $^{229}Th^{3+}$ to its isomeric state $^{229m}Th^{3+}$ via EB. Two lasers at moderate intensity ($(10^{10}-10^{14})$ W/m^2), with photon energies near the optical range, are expected to populate the isomer at a saturated rate of approximately 10^9 s^{-1}, which is much higher than that due to other mechanisms. We believe that this two-photon EB scheme can help in the development of nuclear clocks and deserves verification via a series of experiments with ordinary lasers in laboratories.

Keywords Electronic bridge · ^{229}Th · Nuclear clocks · Two-photon excitation

1 Introduction

Since ancient times, humans have pursued the development of more accurate clocks to arrange social activities and elucidate the secrets of the universe. One of the most important applications of an accurate clock is in global navigation satellite systems, such as the global positioning system (GPS) or BeiDou navigation satellite system (BDS), but they are also used in basic scientific research. Some important units, such as the meter, are defined in relation to a second. Even the time measurement itself would be meaningful, a more precise clock might reveal the intrinsic properties of space and time at the quantum level; e.g., it might be discrete instead of continuous, per the hypothesis of relativity theory.

Currently, atomic or optical clocks are the most accurate time and frequency standards [1]. In 1967, the International System of Units (SI) second was officially redefined based on the isotope atom ^{133}Cs: 'The second is the duration of 9192631770 periods of radiation corresponding to the

This work was supported by the Strategic Priority Research Program of the Chinese Academy of Sciences (No. XDB16) and the Strategic Priority Research Program of the CAS (No. XDB34030000).

✉ Guo-Qiang Zhang
zhangguoqiang@zjlab.org.cn

Chang-Bo Fu
cbfu@fudan.edu.cn

Yu-Gang Ma
mayugang@fudan.edu.cn

[1] ShanghaiTech University, Shanghai 201210, China

[2] Shanghai Institute of Applied Physics, Chinese Academy of Sciences, Shanghai 201800, China

[3] Shanghai Advanced Research Institute, Chinese Academy of Sciences, Shanghai 201210, China

[4] Key Laboratory of Nuclear Physics and Ion-beam Application (MOE), Institute of Modern Physics, Fudan University, Shanghai 200433, China

transition between the two hyperfine levels of the ground state of the cesium 133 atom.' In the following decades, the accuracy of this standard was improved from 10^{-12} (around 100 ns per day) to 10^{-16} [2] because of the significant reduction in the noise-to-signal ratio, with the help of laser cooling. In 2019, scientists from the National Institute of Standards and Technology (NIST) demonstrated an Al^{+} clock with a total uncertainty of 9.4×10^{-19} [3], which is the first demonstration of a clock with an uncertainty of less than 10^{-18}. Recently, atomic clocks based on optical rather than microwave transitions have achieved higher accuracy (2.5×10^{-19}) and stability performance (within 15 s) [4], which might lead to redefining the current cesium microwave-based SI second in the near future.

Despite the great accuracy that atomic and optical clocks have achieved, clocks based on a nuclear transition rather than atomic electron transitions could be more steady and accurate because of their smaller size, with the shielding effects of the surrounding electrons and their higher frequencies. However, nuclei are difficult to control owing to their higher excitation energies (keV to MeV), which have already exceeded those (eV) from modern microwave or laser technologies. Fortunately, two nuclei with excited states lower than 100 eV—i.e., ^{229m}Th (8.10 eV) and ^{235m}U (76 eV)—have been determined thus far. The former has attracted more attention because its transition frequency is closer to the optical range. In 2003, a nuclear optical clock based on a single $^{229}Th^{3+}$ was first proposed by Peik and Tamm [5], although a nuclear transition with an energy of 3.5 eV was much lower than the mean experimental value of 8.10 eV. In their pioneering work, a double-resonance method was proposed with two lasers to excite the nuclear shell and the atomic shell of $^{229}Th^{3+}$, respectively. In 2012, the single $^{229}Th^{3+}$ ion nuclear clock was further investigated by Campbell et al. [6], with a total fractional inaccuracy of 1.0×10^{-19}, which is approximately an order of magnitude higher than that achieved by the best optical atomic clocks at the time. Instead of exciting an electronic shell state, the nuclear clock proposed by Campbell et al. uses a stretched pair of nuclear hyperfine states in the electronic ground-state configuration, which demonstrates advantages with respect to the achievable quality factor and suppression of the quadratic Zeeman shift.

To obtain more precise clocks, an increasing number of proposals for nuclear clocks based on the isomeric isotope ^{229m}Th have been suggested, where the key is how to populate the isomeric state. During the last two decades, various theories have been proposed for populating ^{229}Th to its isomeric state, which can be grouped into laser direct photon excitation, nuclear excitation by electron capture (NEEC), nuclear excitation by electron transition (NEET), and electronic bridges (EB) (see Ref. [7] for a detailed review). Laser direct excitation relies on the precision of the isomeric energy, which has not yet been sufficient. Therefore, indirect excitation schemes—such as NEET, NEEC, and EB—were investigated in alternative ways. NEEC requires a plasma environment to provide free electrons, which seems too harsh to guarantee a low noise level for nuclear clocks. Conversely, NEEC may be a good method for nuclear batteries, such as ^{93}Mo and ^{178}Hf. In the NEET process, a nucleus is excited and a real electronic shell state is simultaneously deexcited, which is a third-order process [7]. Sometimes, it is difficult to distinguish the difference between NEET and EB because they share a similar physics scheme. In Ref. [8], Karpeshin claimed that during NEET processes the virtual level is populated after nuclear excitation, whereas in EB processes, a virtual electronic level is populated before nuclear excitation. Considering all of the theories, it seems that the EB is the most promising for nuclear clocks because of its highly efficient transition rate. Thus far, the uncertainty of the energy isomeric state has seriously hindered the development of nuclear clocks based on ^{229}Th. In the 1970s, the energy was found to be below 100 eV [9] and then below 10 eV in the late 1980s [10]. The energy has shifted from 4.5 ± 1 eV [11] to now 8.10 ± 0.17 eV [12]. Therefore, it was difficult to observe a clear signal from the laser direct excitation experiments. During the EB process, the virtual electronic level tolerates a larger uncertainty of the energy. The EB becomes an important method of populating the ^{229}Th to its isomeric state. Thus, methods based on EB excitation have been proposed during the last decade. In particular, the EB excitation scheme for highly charged $^{229}Th^{35+}$ ions in an EBIT trap was given by Bilous et al. [13].

In this paper, we propose a new theory for calculating the EB excitation rate with two photons for $^{229}Th^{3+}$. We apply the optical Bloch equation for a two-level nuclear system based on an open quantum system and nuclear quantum optics. Taking electrons and nuclei as an effective two-level system during interaction with laser beams and assuming that the system is at equilibrium, we deduce the general formulae for the excitation rate Γ^{eb} and electron bridge enhancement R, respectively. Then, we choose specific atomic shells ($7s - 10s$) as the virtual electronic levels to calculate the transition rates for Th^{3+}. We find that the excitation rate Γ^{eb} and electron bridge enhancement R both reach their maxima when the intensities of the lasers approach the critical value. Moreover, the electron bridge enhancement R should, eventually, be less than one under a relativity intense laser, indicating that populating

the isomeric isotope using a two-photon electronic bridge is not an effective method.

2 Theoretical descriptions

In this section, we deduce a general formalism for two-photon EB excitation. Figure 1a shows the Feynman diagram of a two-photon EB excitation process, where the lower case letters a, b, d, and c denote the atomic shells and g and m indicate the ground and excitation(isomeric) states of the nuclei, respectively. To obtain its expression, one can use the connection between the EB excitation process and the corresponding inverse process of the bound internal conversion (BIC) process [14], as shown in Fig. 1b. This two-photon BIC process can be regarded as a combination of a subprocess one-photon BIC from (a) to (d) and the decay from (d) to (c). Thus, the two-photon BIC rate can be expressed as:

$$\begin{aligned}\Gamma_{\mathrm{bic}}^{(a\to c)} &= \sum_d \Gamma_{\mathrm{bic}}^{(a\to d)}(\Delta_{\mathrm{s}})P^{(d\to c)} \\ &= \sum_d \Gamma_{\mathrm{bic}}^{(a\to d)}(\Delta_{\mathrm{s}})\frac{\Gamma^{(d\to c)}}{\Gamma_d}.\end{aligned} \tag{1}$$

Here, Choosing $\Gamma^{(d\to c)}$ denotes the partial natural decay rate from state (d) to (c) and Γ_d is the total natural decay rate (line width) of state (d). The one-photon BIC is $\Gamma_{\mathrm{bic}}^{(a\to d)} = \sum_b \Gamma_{\mathrm{ic}}^{(a\to b)} \frac{\tilde{\Gamma}_{\mathrm{s}}^2}{\Delta_{\mathrm{s}}^2+\tilde{\Gamma}_{\mathrm{s}}^2}\frac{\Gamma^{(b\to d)}}{\Gamma_b}$, where the frequency difference between the atomic transition and nuclear transition $\Delta_{\mathrm{s}} = \Omega_b - (\Omega_{\mathrm{n}} + \Omega_a)$, where Ω_a, Ω_b, and Ω_{n} are the transition frequencies of (a), (b), and the nucleus. $\tilde{\Gamma}_{\mathrm{s}} = (\Gamma_a + \Gamma_b + \Gamma_{\mathrm{n}})/2$ and $\Gamma_{\mathrm{ic}}^{(a\to b)}$, Γ_a, Γ_b, and Γ_{n} are the widths of the internal conversion (IC) process from (a) to (b), (a), (b), and the isomeric state, respectively [7]. Inserting $\Gamma_{\mathrm{bic}}^{(a\to d)}$ into Eq. (1), we obtain the expression for the two-photon BIC process:

$$\Gamma_{\mathrm{bic}}^{(a\to c)} = \sum_b \sum_d \Gamma_{ic}^{(a\to b)} \frac{\tilde{\Gamma}_{\mathrm{s}}^2}{\Delta_{\mathrm{s}}^2+\tilde{\Gamma}_{\mathrm{s}}^2}\frac{\Gamma^{(b\to d)}}{\Gamma_b}\frac{\Gamma^{(d\to c)}}{\Gamma_d}. \tag{2}$$

One can now obtain the expression of the two-photon EB excitation using the connection between excitation and natural decay rate [14],

$$\Gamma_{\mathrm{exc}}^{\mathrm{eb}\,(c)} = \frac{\pi c^2 I_\ell}{\hbar\left(\Omega_{\mathrm{res}}^{(c)}\right)^3 \tilde{\Gamma}_{\mathrm{res}}^{(c)}}\Gamma_{\mathrm{bic}}^{(c\to a)}. \tag{3}$$

Here, I_ℓ is the intensity of the external laser field. $\Omega_{\mathrm{res}}^{(c)} = \Omega_{\mathrm{n}} + \Omega_c - \Omega_a$ is the EB resonance frequency for the final state (c). $\tilde{\Gamma}_{\mathrm{res}}^{(c)} = \left(\Gamma_{\mathrm{res}}^{(c)} + \Gamma_\ell\right)/2$ is the decoherence rate of the EB resonance. $\Gamma_{\mathrm{res}}^{(c)}$ is the total linewidth of the two-photon EB resonance, obtained as the convolution of the individual linewidths of the atomic and nuclear transitions, $\Gamma_{\mathrm{res}}^{(c)} = \Gamma_{\mathrm{n}} + \Gamma_a + \Gamma_c$.

The partial BIC process rate $\Gamma_{\mathrm{bic}}^{(c\to a)}$ can be obtained by changing the initial and final states (a) and (c) in Eq. (2):

$$\Gamma_{\mathrm{bic}}^{(c\to a)} = \sum_b \sum_d \Gamma_{\mathrm{ic}}^{(c\to b)} \frac{\tilde{\Gamma}_{\mathrm{s}}^2}{\Delta_{\mathrm{s}}^2+\tilde{\Gamma}_{\mathrm{s}}^2}\frac{\Gamma^{(b\to d)}}{\Gamma_b}\frac{\Gamma^{(d\to a)}}{\Gamma_d}. \tag{4}$$

Considering two incident laser beams I_1 and I_2 for the two-photon EB scheme, two factors must be considered:

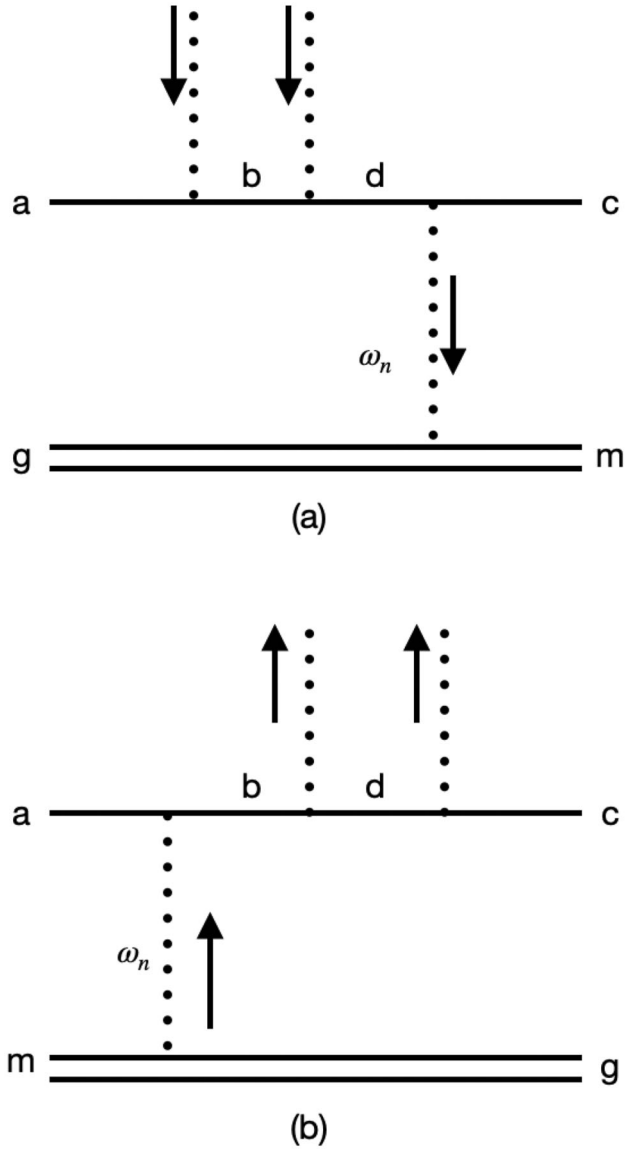

Fig. 1 **a** A two-photon EB process, which absorbs two photons before excitation of the nuclei. **b** A two-photon bound internal conversion (BIC) process, which emits two photons after deexcitation of the nuclei

$\frac{\pi c^2 I_1}{\Omega_s^3 \tilde{\Gamma}_s}, \frac{\pi c^2 I_2}{\Omega_{res}^3 \tilde{\Gamma}_{res}}$. Thus, one obtains the proper formula for the two-photon EB excitation rate from Eq. (3),

$$\Gamma_{exc}^{eb\,(c)} = \frac{\pi c^2 I_1}{\hbar\left(\Omega_s^{(c)}\right)^3 \tilde{\Gamma}_s^{(c)}} \frac{\pi c^2 I_2}{\hbar\left(\Omega_{res}^{(c)}\right)^3 \tilde{\Gamma}_{res}^{(c)}} \frac{\tilde{\Gamma}_{s_2}^2}{\Delta_{s_2}^2 + \tilde{\Gamma}_{s_2}^2} \Gamma_{bic}^{(c\to a)}. \tag{5}$$

Inserting Eq. (4) into Eq. (5) and exchanging (b) and (d), we obtain

$$\Gamma_{exc}^{eb\,(c)} = \sum_b \sum_d \frac{\pi c^2 I_1}{\hbar\left(\Omega_s^{(c)}\right)^3 \tilde{\Gamma}_s^{(c)}} \frac{\pi c^2 I_2}{\hbar\left(\Omega_{res}^{(c)}\right)^3 \tilde{\Gamma}_{res}^{(c)}} \frac{\tilde{\Gamma}_{s_2}^2}{\Delta_{s_2}^2 + \tilde{\Gamma}_{s_2}^2} \Gamma_{ic}^{(c\to d)} \frac{\tilde{\Gamma}_s^2}{\Delta_s^2 + \tilde{\Gamma}_s^2} \frac{\Gamma^{(d\to b)}}{\Gamma_b} \frac{\Gamma^{(b\to a)}}{\Gamma_d}. \tag{6}$$

Here $\Omega_s = \Omega_b - \Omega_a$, $\Delta_s = \Omega_1 - (\Omega_b - \Omega_a)$, $\Delta_{s_2} = \Omega_2 - \Omega_d + \Omega_b$, $\Gamma_{s_2} = \Gamma_d + \Gamma_b$, $\Gamma_s = \Gamma_b + \Gamma_a$, $\tilde{\Gamma}_s = (\Gamma_s + \Gamma_1)/2$, $\Omega_{res} = \Omega_n + \Omega_c - \Omega_b$, $\Gamma_{ic}^{(c\to d)}$ is the IC process from (c) to (d). The IC process $\Gamma_{ic}^{(c\to d)}$ takes the form of Eq. [15]

$$\Gamma_{ic}^{(c\to d)} = \frac{\alpha_d^{(c\to d)} \Gamma_\Gamma}{\Gamma_d}, \tag{7}$$

where $\alpha_d^{(c\to d)}$ is the internal conversion coefficient. If only the bound states for both the initial and final electron states, a and c, are considered, Eq. (6) becomes

$$\Gamma_{exc}^{eb\,(c)} = \sum_b \sum_d \frac{\pi c^2 I_1}{\hbar\left(\Omega_s^{(c)}\right)^3 \tilde{\Gamma}_s^{(c)}} \frac{\pi c^2 I_2}{\hbar\left(\Omega_{res}^{(c)}\right)^3 \tilde{\Gamma}_{res}^{(c)}} \frac{\tilde{\Gamma}_{s_2}^2}{\Delta_{s_2}^2 + \tilde{\Gamma}_{s_2}^2} \frac{\alpha_d^{(c\to d)} \Gamma_\Gamma}{\Gamma_d} \frac{\tilde{\Gamma}_s^2}{\Delta_s^2 + \tilde{\Gamma}_s^2} \frac{\Gamma^{(d\to b)}}{\Gamma_b} \frac{\Gamma^{(b\to a)}}{\Gamma_d}. \tag{8}$$

In this study, we follow Ref. [7], which takes the nuclear ground and excited states as a two-level quantum system in an external laser field. The corresponding evolution density matrix for this system is

$$\hat{\rho}(t) = \rho_{ee}|e\rangle\langle e| + \rho_{ge}|g\rangle\langle e| + \rho_{eg}|e\rangle\langle g| + \rho_{gg}|g\rangle\langle g|. \tag{9}$$

Here, $|g\rangle$ and $|e\rangle$ are the ground and excited states, respectively. The population density $\rho_{exc}(t)$ under resonant laser irradiation can be modeled using Torrey's solution of the optical Bloch equations [16]. The Rabi frequency Ω_{eg} for the nuclear transition is introduced as in [16]

$$\Omega_{eg}^2 = 2\Gamma_{exc}^{\Gamma} \tilde{\Gamma}_n = \frac{2\pi c^2 I_\ell \Gamma_\Gamma}{\hbar \Omega_n^3}, \tag{10}$$

where Γ_{exc}^{Γ} is the excitation rate. $\tilde{\Gamma}_n = \Gamma_\Gamma + \Gamma_{nr}$ is the total width of the nuclear transition, including Γ decay (Γ_Γ) and other non-radiative decay channels (Γ_{nr}). Similarly, to calculate the two-photon EB process using this nuclear quantum optics, we define the Rabi frequency for the EB process as $\Omega_{eb}^{(c)\,2} = 2\Gamma_{exc}^{eb\,(c)} \tilde{\Gamma}_{res}^{(c)}$, which can be used to model the on-resonance nuclear population density as a function of time for EB excitation when substituting Ω_{eg} for $\Omega_{eb}^{(c)}$ and $\tilde{\Gamma}_n$ for $\tilde{\Gamma}_{res}^{(c)}$ in Eq. (10). In the following, we extend a low saturation limit approximation to a general case.

2.1 Low saturation limit

Assuming that the intensity of the laser is sufficiently low (so that the excited state is far less populated than the ground state), the solution for the optical Bloch equation is [16]

$$\rho_{exc}^{eb} \equiv \rho_{ee} = \frac{\Omega_{eg}^2 \tilde{\Gamma}_n/(2\Gamma_n)}{(\Delta\Omega)^2 + \tilde{\Gamma}_n^{\,2}} \left(1 - e^{-\Gamma_n t}\right). \tag{11}$$

Given sufficient time, t, the system evolves; when the population of the excited state is in equilibrium, i.e., the excitation rate is equal to the total decay rate, the total decay rate can be expressed as a product of the population density and the natural decay rate:

$$\rho_{exc}^{eb} \equiv \rho_{ee} \to \frac{\Omega_{eg}^2 \tilde{\Gamma}_n/(2\Gamma_n)}{\Delta_n^2 + \tilde{\Gamma}_n^2} = \Gamma_{exc}^{\Gamma} \frac{\tilde{\Gamma}_n^2/\Gamma_n}{\Delta_n^2 + \tilde{\Gamma}_n^2}. \tag{12}$$

With nonzero detuning $\Delta_{res}^{(c)}$ of the laser light with respect to the EB resonance, we can obtain

$$\Gamma_{exc}^{eb}(\Delta_{res}) = \rho_{exc}^{eb}(\Delta_{res})\Gamma_n = \Gamma_{exc}^{eb}(0) \frac{\tilde{\Gamma}_{res}^2}{\Delta_{res}^2 + \tilde{\Gamma}_{res}^2}. \tag{13}$$

Inserting Eq. (8) into Eq. (13), an additional factor $\frac{\tilde{\Gamma}_{res}^2}{\Delta_{res}^2 + \tilde{\Gamma}_{res}^2}$ for the EB excitation rate at a low saturation limit.

$$\begin{aligned}\Gamma_{\mathrm{ls}}^{\mathrm{eb}} &\equiv \Gamma_{\mathrm{exc}}^{\mathrm{eb}}(\Delta_{\mathrm{res}}) \\ &= \sum_b \sum_d \frac{\pi c^2 I_1}{\hbar\left(\Omega_{\mathrm{s}}^{(c)}\right)^3 \tilde{\Gamma}_{\mathrm{s}}^{(c)}} \\ &\quad \frac{\pi c^2 I_2}{\hbar\left(\Omega_{\mathrm{res}}^{(c)}\right)^3 \tilde{\Gamma}_{\mathrm{res}}^{(c)}} \frac{\tilde{\Gamma}_{\mathrm{s2}}^2}{\Delta_{\mathrm{s2}}^2 + \tilde{\Gamma}_{\mathrm{s2}}^2} \frac{\alpha_d^{(c\to d)}\Gamma_\Gamma}{\Gamma_d} \frac{\tilde{\Gamma}_{\mathrm{s}}^2}{\Delta_{\mathrm{s}}^2 + \tilde{\Gamma}_{\mathrm{s}}^2} \frac{\Gamma^{(d\to b)}}{\Gamma_b} \\ &\quad \frac{\Gamma^{(b\to a)}}{\Gamma_d} \frac{\tilde{\Gamma}_{\mathrm{res}}^2}{\Delta_{\mathrm{res}}^2 + \tilde{\Gamma}_{\mathrm{res}}^2}\end{aligned} \tag{14}$$

here the (c) index was dropped for easier notation and $\Delta_{\mathrm{res}} = \Omega_2 - \Omega_{\mathrm{res}} = \Omega_2 - \Omega_{\mathrm{n}} - \Omega_c + \Omega_b$.

Note that this equation is similar to that in [7] and others [8, 14] but our formula does not require a certain excited electronic state (b). An interesting feature of the low-limit saturation two-photon EB excitation is its double resonance effect. When $\Delta_{\mathrm{s}} = 0$ is satisfied in the system, one will obtain $\Delta_{\mathrm{res}} = 0$ and vice versa. At resonance $\Delta_{\mathrm{s}} = 0$, $\Delta_{\mathrm{res}} = 0$, when $a = 7s$, $c = 7s$, $b = 7p_{1/2}$, $d = 8s$, $I_1 = I_2 \equiv I = 3 \times 10^5$ W/m^2, $\Gamma_1 = 10^{-5}$ eV are satisfied, we obtain $\Gamma_{\mathrm{exc}}^{\mathrm{eb}} = 0.082\ \mathrm{s}^{-1}$, which is comparable to the results reported in [8, 14], where the values of 10 s^{-1} and 0.0281 s^{-1} for Th^+ were obtained, respectively.

For convenience, considering two incident lasers with the same laser intensity $I_1 = I_2 \equiv I$, the EB enhancement coefficient R can be defined as the ratio between the EB excitation cross section and the direct photon excitation cross-section.

$$R_{\mathrm{eb}}^{(c)} = \frac{\sigma_{\mathrm{eb}}^{(c)}}{\sigma_\Gamma} \simeq \frac{\Gamma_{\mathrm{exc}}^{\mathrm{eb}\,(c)}}{\Gamma_{\mathrm{exc}}^{\Gamma}} \tag{15}$$

Here, $\Gamma_{\mathrm{exc}}^{\mathrm{eb}\,(c)}$ denotes the EB-excitation rate at resonance, and $\Gamma_{\mathrm{exc}}^{\Gamma}$ is the excitation rate for direct photon excitation [7]:

$$\Gamma_{\mathrm{exc}}^{\Gamma} = \frac{\sigma_\Gamma I_\ell}{\hbar\Omega_{\mathrm{n}}} = \frac{\pi c^2 I_\ell}{\hbar\Omega_{\mathrm{n}}^3 \tilde{\Gamma}_{\mathrm{n}}} \Gamma_\Gamma. \tag{16}$$

Here, $\tilde{\Gamma}_n = (\Gamma_{\mathrm{n}} + \Gamma_l)/2$. Inserting Eqs. (14) and (16) into Eq. (15), one can obtain the enhancement coefficient for two-photon EB excitation at a low saturation limit:

$$\begin{aligned}R_{\mathrm{ls}}^{(b)} &= \sum_d \left(\frac{\Omega_{\mathrm{n}}}{\Omega_{\mathrm{s}}}\right)^3 \left(\frac{\tilde{\Gamma}_{\mathrm{n}}}{\tilde{\Gamma}_{\mathrm{s}}}\right)^3 \\ &\quad \frac{\pi c^{2I}}{\Omega_{\mathrm{res}}^3 \tilde{\Gamma}_{\mathrm{res}}} \frac{\tilde{\Gamma}_{\mathrm{s}_2}^2}{\Delta_{\mathrm{s}_2}^2 + \tilde{\Gamma}_{\mathrm{s}_2}^2} \\ &\quad \frac{\alpha_d^{(c\to d)}}{\Gamma_d} \frac{\Gamma^{(d\to b)}}{\Gamma_d} \frac{\Gamma^{(b\to a)}}{\Gamma_b} \frac{\tilde{\Gamma}_{\mathrm{s}}^2}{\Delta_{\mathrm{s}}^2 + \tilde{\Gamma}_{\mathrm{s}}^2} \frac{\tilde{\Gamma}_{\mathrm{res}}^2}{\Delta_{\mathrm{res}}^2 + \tilde{\Gamma}_{\mathrm{res}}^2}.\end{aligned} \tag{17}$$

Here, the (c) index was dropped for easier notation and the subscript 'ls' indicates the low saturation limit. At resonance $\Delta_{\mathrm{s}} = 0$, $\Delta_{\mathrm{res}} = 0$, and we obtain

$$\begin{aligned}R_{\mathrm{ls}}^{(b)} &= \sum_d \left(\frac{\Omega_{\mathrm{n}}}{\Omega_{\mathrm{l}}}\right)^3 \left(\frac{\tilde{\Gamma}_{\mathrm{n}}}{\tilde{\Gamma}_{\mathrm{s}}}\right)^3 \frac{\pi c^{2I}}{\Omega_2^3 \tilde{\Gamma}_{\mathrm{s}}} \\ &\quad \times \frac{\tilde{\Gamma}_{\mathrm{s}_2}^2}{\Delta_{\mathrm{s}_2}^2 + \tilde{\Gamma}_{\mathrm{s}_2}^2} \frac{\alpha_d^{(c\to d)}}{\Gamma_d} \frac{\Gamma^{(d\to b)}}{\Gamma_d} \frac{\Gamma^{(b\to a)}}{\Gamma_b}.\end{aligned} \tag{18}$$

2.2 General case

When the laser beam is sufficiently large or there is a double resonance effect, the excitation rate is large. In this case, the low saturation limit can no longer provide a good prediction. Then, the general steady-state solution of the optical Bloch equation is adopted [16]

$$\rho_{\mathrm{ee}} = \frac{\Omega_{\mathrm{eg}}^2}{\frac{2\Gamma}{\tilde{\Gamma}}\left((\Delta\Omega)^2 + \tilde{\Gamma}^2\right) + 2\Omega_{\mathrm{eg}}^2}. \tag{19}$$

Using the same procedure from quantum opticals as in the low saturation limit, $\Omega_{\mathrm{eg}} \to \Omega_{\mathrm{eb}}$, $\tilde{\Gamma}_{\mathrm{n}} \to \tilde{\Gamma}_{\mathrm{res}}$

$$\begin{aligned}\Gamma^{\mathrm{eb}(g)} &= \sum_b \rho_{\mathrm{exc}}^{\mathrm{eb}(g)(b)} \Gamma_{\mathrm{n}} \\ &= \sum_b \frac{\Gamma_{\mathrm{ls}}^{\mathrm{eb}}(0)\tilde{\Gamma}_{\mathrm{res}}\Gamma_{\mathrm{res}}}{\frac{\Gamma_{\mathrm{res}}}{\tilde{\Gamma}_{\mathrm{res}}}\left(\Delta_{\mathrm{res}}^2 + \tilde{\Gamma}_{\mathrm{res}}^2\right) + 2\Gamma_{\mathrm{ls}}^{\mathrm{eb}}(0)\tilde{\Gamma}_{\mathrm{res}}}.\end{aligned} \tag{20}$$

At resonance, $\Delta_{\mathrm{res}} = 0$, $\Delta_{\mathrm{s}_1} = 0$, and the electronic excited state (b) is fixed. Considering $I_1 = I_2 \equiv I$, we obtain

$$\Gamma^{\mathrm{eb}(g)(b)} = \frac{\Gamma_{\mathrm{exc}}^{\mathrm{eb(ls)(b)}}}{1 + 2\Gamma_{\mathrm{exc}}^{\mathrm{eb(ls)(b)}} \frac{1}{\tilde{\Gamma}_{\mathrm{res}}}}, \tag{21}$$

$$R_{\mathrm{eb}}^{(b)} = \frac{R_{\mathrm{ls}}^{(b)}}{1 + 2\frac{\Gamma_\Gamma}{\tilde{\Gamma}_{\mathrm{res}}} \sum_d \frac{\pi c^2 I}{\Omega_{\mathrm{l}}^3 \tilde{\Gamma}_{\mathrm{s}}} R^{(d)\prime}}, \tag{22}$$

where superscript 'g' indicates general excitation and

$$R_{\mathrm{ls}}^{(b)} = \sum_{d}\left(\frac{\Omega_{\mathrm{n}}}{\Omega_{\mathrm{l}}}\right)^{3}\left(\frac{\tilde{\Gamma}_{\mathrm{n}}}{\tilde{\Gamma}_{\mathrm{s}}}\right)^{3}\frac{\pi c^{2} I}{\Omega_{2}^{3}\tilde{\Gamma}_{\mathrm{s}}}\frac{\tilde{\Gamma}_{\mathrm{s}_2}^{2}}{\Delta_{\mathrm{s}_2}^{2}+\tilde{\Gamma}_{\mathrm{s}_2}^{2}} \times \frac{\Gamma_{\mathrm{ic}}^{(c\to d)}}{\Gamma_{\Gamma}}\frac{\Gamma^{(d\to b)}}{\Gamma_{d}}\frac{\Gamma^{(b\to a)}}{\Gamma_{b}}, \tag{23}$$

$$R^{(d)\prime} = \frac{\pi c^{2} I}{\Omega_{2}^{3}\tilde{\Gamma}_{\mathrm{res}}}\frac{\tilde{\Gamma}_{\mathrm{s}_2}^{2}}{\Delta_{\mathrm{s}_2}^{2}+\tilde{\Gamma}_{\mathrm{s}_2}^{2}}\frac{\Gamma_{ic}^{(c\to d)}}{\Gamma_{\Gamma}}\frac{\Gamma^{(d\to b)}}{\Gamma_{d}}\frac{\Gamma^{(b\to a)}}{\Gamma_{b}}. \tag{24}$$

It seems that the general formalism for $\Gamma^{\mathrm{eb}(g)(b)}$ is simply multiplied by a decay factor, such as $\frac{1}{1+2\Gamma_{\mathrm{exc}}^{\mathrm{eb(ls)(b)}}\frac{1}{\Gamma_{\mathrm{res}}}}$ and is similar to R. Therefore, we may have a maximum for both $\Gamma^{\mathrm{eb}(g)(b)}$ and R, as presented in the next section. Note that this is a general result and, in this work, we use it to calculate Th^{3+}.

3 Results and discussion

First, we set up some parameters before performing the calculations. Recently, an energy of 8.10 ± 0.17 eV for $^{229\mathrm{m}}$Th was obtained [12], which has the same precision as the value obtained from IC spectroscopy [17]. Generally, the radiative decay rate $\Gamma_{\Gamma} = 1/\tau_{\Gamma}$ of magnetic multipole transitions can be expressed in terms of the energy-independent reduced transition probability $B_{\downarrow}(ML)$, as in [18]

$$\Gamma_{\Gamma} = \frac{2\mu_0}{\hbar}\frac{L+1}{L[(2L+1)!!]^2}\left(\frac{\Omega_{\mathrm{n}}}{c}\right)^{2L+1} B_{\downarrow}(ML). \tag{25}$$

Here, L denotes multipolarity and Ω_{n} is the angular frequency of the nuclear transition. However, in this study, we choose $B_{\downarrow}(ML) = 5.0 \times 19^{-3}$ W.u. and $\tau_{\Gamma} = 1.2 \times 10^{4}$ s, as in Ref. [19]. The width of the laser is approximately $\Gamma_{\mathrm{l}} = 10^{-5}$ eV. The energy spectrum of the valence electron is obtained from experiments by Blaise and Wyart [20]. Transition rates, such as $\Gamma^{(c\to d)}$, and lifetimes for different intermediate states are from [21, 22], which considers $^{229}Th^{3+}$ to be a Fr-like atom. Because of the metastability and long lifetime of 7s, $\tau_{7s} = 0.6$ s in Ref. [22], we chose $7s$ as the initial state (a). The electronic shell can be effectively transferred from the ground state $5F_{5/2}$ to the 7s state by making use of the Stimulated Raman Adiabatic Passage (STIRAP) method [23] via the intermediate state $6d_{3/2}$ and more details about STIRAP are in Ref. [24]. In addition, we make use of the fact (also considered in [25]) that the coupling of the nuclear transition is maximal to an $M1$ electronic transition between s orbitals; thus, ns $(n = 7, 8, 9, 10)$ for the final state (c) is considered. To obtain $\alpha_{d}^{(c\to d)}$ an $M1$ electronic transition, the ns $(n = 7, 8, 9, 10)$ atomic shells are only considered for (d). Furthermore, from Eq. (13), two factors $\Gamma^{(b\to a)}$ and $\Gamma^{(d\to b)}$ indicate that state (b) should be np_j $(n = 7, 8, 9, 10)$, $(j = 1/2, 3/2)$ to make $E1$ transitions between them. For a detailed analysis of the results, we divided this section into three parts: a small laser ($(10^4$–$10^{10})$ W/m^2), moderate laser($(10^{10}$–$10^{14})$ W/m^2), and strong laser ($\geq 10^{18}$ W/m^2).

3.1 Small laser

Figure 2a shows the relationship between the two-photon EB enhancement R and laser intensity I. The diagram in Fig. 2b is divided into three parts, i.e., the small laser ($(10^4$–$10^{10})$ W/m^2), moderate laser ($(10^{10}$–$10^{14})$ W/m^2), and strong laser ($\geq 10^{18}$ W/m^2). Figure 3 shows the two-photon EB excitation rate Γ^{eb} as a function of the laser intensity I. Here, R_1 indicates EB enhancement using atomic shell $a = 7s, b = 7p_{1/2}, c = 7s$. R_2 stands for $a = 7s, b = 7p_{3/2}, c = 7s$, R_3 is $a = 7s, b = 7p_{1/2}, c = 8s$. R_4 is $a = 7s, b = 7p_{3/2}, c = 8s$, R_5 is

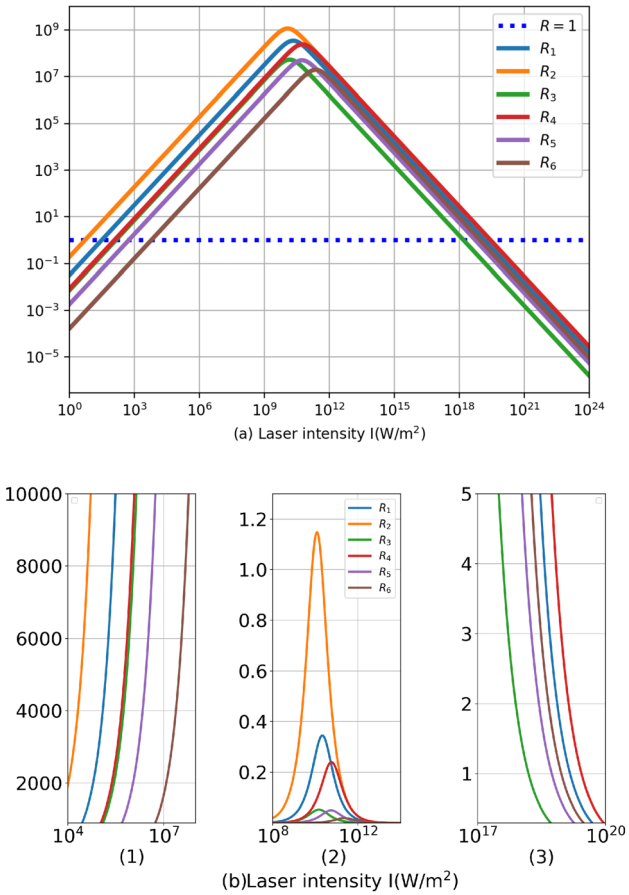

Fig. 2 **a** Two-photon EB process enhancement factor R as a function of laser intensity I for different atomic shells (b), (c). The dashed line indicates a factor of one. **b** Three cases for the laser intensity at different atomic shells $((b), (c)$. The y value in subplot(2) is normalized to 10^9

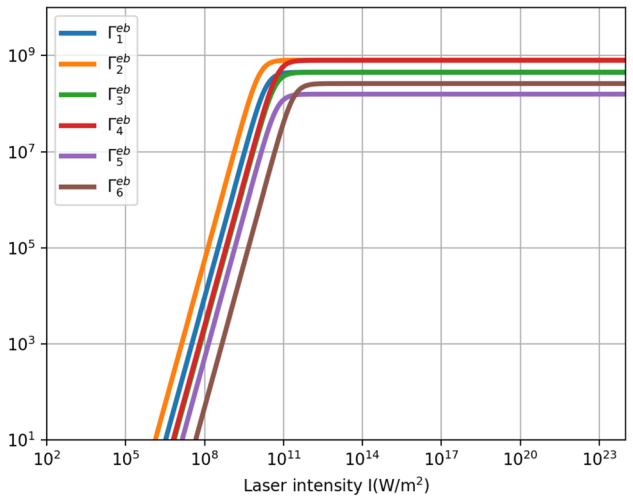

Fig. 3 Relationship between two-photon EB excitation rate Γ^{eb} and laser intensity I for different atomic shells (b) (c)

$a = 7s, b = 8p_{1/2}, c = 8s$, and R_6 is $a = 7s, b = 8p_{3/2}, c = 8s$. These notations are the same for Γ^{eb}. We see that both R and Γ^{eb} increase with increasing laser intensity. Surprisingly, from Fig. 3, we note that the excitation rate of the nuclei is only large for a moderate intensity laser, e.g., $I \sim 10^8$ W/m^2. For example, when we choose $a = 7s, b = 7p_{1/2}, c = 7s$ as our atomic shell, from Table 1, the photon energies of the two laser beams are $\Omega_1 = 4.6008$ eV and $\Omega_2 = 3.4992$ eV, respectively. The wavelengths are $\lambda_1 = 269.02$ nm, $\lambda_2 = 353.57$ nm, which are close to the optical range. Assuming equilibrium, the corresponding EB enhancement R_1 and excitation rate Γ_1^{eb} are

$$R_1 = \frac{0.0322I}{2.18 \times 10^{-21} I^2 + 1}, \tag{26}$$

$$\Gamma_1^{eb} = \frac{9.29 \times 10^{-13} I^2}{1 + 2.04 \times 10^{-21} I^2}. \tag{27}$$

Table 1 Laser intensity I_0 when the two-photon EB excitation enhancement factor R reaches its maximum with corresponding excitation Γ^{eb}, incident laser energies Ω_1,Ω_2 at different atomic shells (b), (c) but for the same initial state $(a) = 7s$

(b)	(c)	Ω_1 (eV)	Ω_2 (eV)	$\Gamma^{eb}(10^8$ s$^{-1})$	$R(10^8)$	I_0[a]
$7p_{1/2}$	7s	4.6008	3.4992	2.17	3.45	1.20
$7p_{3/2}$	7s	6.1899	1.9101	3.96	11.5	1.19
$7p_{1/2}$	8s	4.6008	15.459	2.27	1.68	4.68
$7p_{3/2}$	8s	6.1899	13.870	3.97	2.40	5.72
$8p_{1/2}$	8s	13.810	6.2500	0.78	0.50	5.50
$8p_{3/2}$	8s	14.474	5.5860	1.32	0.18	23.5

[a]Here, the unit for laser intensity is 10^{10} W/m^2

Choosing $I = 10^7$ W/m^2, from Eqs.(26) and (27), one can obtain $R_1 = 3.22 \times 10^5$, $\Gamma_1^{eb} = 92.9$ s^{-1}, which is similar to the result 10 s^{-1} for Th^+ in Ref. [14], where a laser pulses with 10 mJ energy and a spectral width of $\Delta\Omega = 2\pi\times$ 3 GHz, at a repetition rate of 30 Hz and focusing to a spot size of 0.1 mm; hence, their excitation rate of $\Gamma^{eb} = 10$ s^{-1}. Alternatively, if we let $I = 9 \times 10^5$ W/m^2, then we obtain $\Gamma_1^{eb} = 0.75$ s^{-1} , $R_1 = 2.89 \times 10^4$, and in [8] the excitation rate $\Gamma^{eb} = 0.0281$ s^{-1} for Th^+. It is interesting to note that the result $R_1 = 3.22\times 10^5$ is comparable with the result of $10 \rightarrow 10^6$ of one-photon EB in the low saturation case [7].

3.2 Moderate laser

Usually, owing to the low-excitation cross section of the nuclei, a low saturation limit for excitation is assumed and satisfied in most cases. However, in this work, cross-sections from the two-photon EB excitation under resonance conditions are quite large so that the low saturation limit will no longer be satisfied. We extend the low saturation limit to a general situation, including the large excitation case for the first time, as shown in the general case of the theoretical descriptions. We find that the two-photon EB enhancement R reaches its maximum when $I = I_0$ is satisfied. From Fig. 1b and Table (1), we see that R_2 has the largest value, i.e., $R_2 = 1.15 \times 10^9$ when $I_0 = 1.19 \times 10^{10}$ W/m^2. At the same time, the excitation rate Γ^{eb} also has a maximum value, as shown in Fig. 3. Surprisingly, at a certain point, the excitation rate Γ^{eb} increases very slowly as the intensity I increases; we refer to this point as I_0'. It is quite amazing that when $I \sim 10^{10}$ W/m^2, we obtain $R \sim 10^8$; however, note that we only consider the case of $\Delta_s = 0$ and $\Delta_{res} = 0$. If the conditions ($\Delta_{s_2} = 0$ but $\Delta_s \neq 0$ and $\Delta_{res} \neq 0$) are satisfied, from Eq. (17), there are two extra resonant factors, namely $\frac{\tilde{\Gamma}_{res}^2}{\Delta_{res}^2+\tilde{\Gamma}_{res}^2}$, $\frac{\tilde{\Gamma}_s^2}{\Delta_s^2+\tilde{\Gamma}_s^2}$. Thus, one can obtain

$$R_{ls}^{(b)} = \sum_b \sum_d \left(\frac{\Omega_n}{\Omega_1}\right)^3 \left(\frac{\tilde{\Gamma}_n}{\tilde{\Gamma}_s}\right)^3 \frac{\pi c^2 I}{\Omega_2^3 \tilde{\Gamma}_s} \frac{\alpha_d^{(c\rightarrow d)}}{\Gamma_d} \frac{\Gamma^{(d\rightarrow b)}}{\Gamma_d} \times \frac{\Gamma^{(b\rightarrow a)}}{\Gamma_b} \frac{\tilde{\Gamma}_s^2}{\Delta_s^2 + \tilde{\Gamma}_s^2} \frac{\tilde{\Gamma}_{res}^2}{\Delta_{res}^2 + \tilde{\Gamma}_{res}^2}. \tag{28}$$

Assuming $\Gamma_1 = 10^{-5}$ eV, and $\Delta_s, \Delta_{res} \sim$ eV, $\tilde{\Gamma}_s \sim \Gamma_1$, $\tilde{\Gamma}_{res} \sim \Gamma_1$, one obtains the two resonant factors $\frac{\Gamma_1^2}{\Delta_s^2}$, and $\frac{\Gamma_1^2}{\Delta_{res}^2}$, respectively. Thus, Eq. (28) becomes

$$R_{\rm ls}^{(b)} = \sum_b \sum_d \left(\frac{\Omega_{\rm n}}{\Omega_{\rm l}}\right)^3 \left(\frac{\tilde{\Gamma}_{\rm n}}{\tilde{\Gamma}_{\rm s}}\right)^3 \frac{\pi c^2 I}{\Omega_2^3 \tilde{\Gamma}_{\rm s}} \frac{\alpha_d^{(c\to d)}}{\Gamma_d} \frac{\Gamma^{(d\to b)}}{\Gamma_d} \frac{\Gamma^{(b\to a)}}{\Gamma_b} \frac{\Gamma_{\rm l}^2}{\Delta_{\rm s}^2} \frac{\Gamma_{\rm l}^2}{\Delta_{\rm res}^2}. \tag{29}$$

In this case, it is quite clear that the threshold will be 10^{10} times larger than the low saturation limit, as shown in Eq. (18), indicating that a stronger laser field is required to reach a larger EB excitation rate.

3.3 Strong laser

We notice that when the intensity of the laser reaches I_0', the excitation rate $\Gamma^{\rm eb}$ saturates as the intensity I increases. As the intensity increases, the EB enhancement factor R will eventually be less than one because of the rapid increase in $\Gamma_{\rm exc}^{\Gamma}$. Figure 2a demonstrates this tendency. When the intensity of the laser reaches $I \sim (10^{19} - 10^{20})$ W/m^2, one obtains $R \sim 1$. The case of $R < 1$ is common in the literature. For example, in Ref. [26], they choose an initial electron state $i = 5f_{5/2}$ and a final electron state $f = 6d_{3/2}, 6d_{5/2}, 7s_{1/2}$. In these cases, the EB enhancement factors β are 0.015, 0.0015, and 2×10^{-9}, respectively. Note that the case of $R < 1$ is shell-independent in our situation, it will eventually be less than one. To see this, from Eq. (22), we obtain

$$\begin{aligned} R_{\rm eb}^{(g)(b)} &= \frac{R_{\rm ls}^{(b)}}{1 + 2\frac{\Gamma_\Gamma}{\Gamma_{\rm res}} \sum_d \frac{\pi c^2 I}{\Omega_1^3 \tilde{\Gamma}_{\rm s}} R^{(d)\prime}} \\ &= \frac{R_{\rm ls}^{(b)}}{1 + 2\frac{\Gamma_\Gamma}{\Gamma_{\rm res}} \left(\frac{\Omega_{\rm n}}{\Omega_{\rm l}}\right)^3 \left(\frac{\tilde{\Gamma}_{\rm n}}{\tilde{\Gamma}_{\rm s}}\right)^3 \sum_d \frac{\pi c^2 I}{\Omega_1^3 \tilde{\Gamma}_{\rm s}} R^{(d)\prime}} \end{aligned} \tag{30}$$

from Eqs. (23) and (24), one can obtain

$$R_{\rm ls}^{(b)} = \sum_d \left(\frac{\Omega_{\rm n}}{\Omega_{\rm l}}\right)^3 \left(\frac{\tilde{\Gamma}_{\rm n}}{\tilde{\Gamma}_{\rm s}}\right)^3 R^{(d)\prime}. \tag{31}$$

Thus, Eq. (32) becomes

$$R_{\rm eb}^{(g)(b)} = \frac{R_{\rm ls}^{(b)}}{1 + 2\frac{\Gamma_\Gamma}{\Gamma_{\rm res}} \frac{\pi c^2 I}{\Omega_1^3 \tilde{\Gamma}_{\rm s}} R_{\rm ls}^{(b)}}. \tag{32}$$

From Eq. (23), we obtain a linear dependence on the laser intensity in the low saturation case, $R_{\rm ls}^{(b)} \sim I$ while, at a strong laser intensity from Eq. (32), we obtain $R_{\rm eb}^{(g)(b)} \sim a_1 I/(1 + b_1 I^2)$, which is no longer linear. When the condition $I \to \infty$ is satisfied, then one obtains $R_{\rm eb}^{(g)(b)} \sim 0$. At an intensity $\sim (10^{19} - 10^{20})$ W/m^2, the two-photon EB process is not an effective method of exciting nuclei. Generally, it is difficult to determine whether an EB process is effective but we see that, at high laser intensity, the two-photon EB process is not an effective method. In this case, the direct photonuclear excitation rate dominates. Actually, we do not include any field or nonlinear effects in this calculation, which should be an interesting task in the future.

4 Summary

In summary, we propose a two-photon EB excitation scheme to populate the isomeric isotope $^{229m}Th^{3+}$. Based on the nuclear quantum optics for two-level open quantum systems, we deduce an expression for the two-photon EB excitation rate in an electron-nucleus system. The nuclear excitation rate $\Gamma^{\rm eb}$ and its efficiency R were derived under equilibrium conditions. Using the experimentally-known energy levels of $^{229}Th^{3+}$, we obtained the EB excitation rate of $^{229}Th^{3+}$ and the efficiency R as a function of laser intensity. Three cases of laser intensity were investigated: a small laser ($(10^4$–$10^{10})$ W/m^2), moderate laser near the critical ($(10^{10}$–$10^{14})$ W/m^2), and strong laser ($\geq 10^{18}$ W/m^2). We find that near the critical value ($(10^{10}$–$10^{14})$ W/m^2), the nuclear excitation rate $\Gamma^{\rm eb}$, and the electronic bridge efficiency R reach their maximum values under a strong laser ($\geq 10^{18}$ W/m^2), the two-photon electronic bridge efficiency R will eventually be less than one. In this calculation, we do not consider the hyperfine structure due to electromagnetic splitting, which will be conducted in future work. We believe that this two-photon EB scheme can help to realize nuclear clocks and suggest verifying the scheme through a series of experiments with ordinary lasers in laboratories.

References

1. A.D. Ludlow, M.M. Boyd, J. Ye et al., Optical atomic clocks. Rev. Mod. Phys. **87**, 637 (2015). https://doi.org/10.1103/RevModPhys.87.637
2. C. Audoin, B. Guinot, S. Lyle, *The Measurement of Time: Time, Frequency and the Atomic Clock* (Cambridge University Press, Cambridge, 2001), pp. 51–56
3. S.M. Brewer, J.-S. Chen, A.M. Hankin et al., $^{27}Al^+$ Quantum-logic clock with a systematic uncertainty below 10^{-18}. Phys. Rev. Lett. **123**, 033201 (2019). https://doi.org/10.1103/PhysRevLett.123.033201
4. G.E. Marti, R.B. Hutson, A. Goban et al., Imaging optical frequencies with 100μ Hz precision and 1.1μm resolution. Phys. Rev. Lett. **120**, 103201 (2018). https://doi.org/10.1103/PhysRevLett.120.103201
5. E. Peik, C. Tamm, Nuclear laser spectroscopy of the 3.5 eV transition in Th-229. Eur. Phy. Lett. **61**, 181 (2003). https://doi.org/10.1209/epl/i2003-00210-x

6. C.J. Campbell, A.G. Radnaev, A. Kuzmic et al., Single-ion nuclear clock for metrology at the 19th decimal place. Phys. Rev. Lett. **108**, 120802 (2012). https://doi.org/10.1103/PhysRevLett.108.120802
7. L. Wense, B. Seiferle, The ^{229}Th isomer: prospects for a nuclear optical clock. Eur. Phys. J. A **56**, 277 (2020). https://doi.org/10.1140/epja/s10050-020-00263-0
8. F.F. Karpeshin, M.B. Trzhaskovskaya, Bound internal conversion versus nuclear excitation by electron transition: Revision of the theory of optical pumping of the ^{229m}Th isomer. Phys. Rev. C **95**, 034310 (2017). https://doi.org/10.1103/PhysRevC.95.034310
9. L.A. Kroger, C.W. Reich, Features of the low energy level scheme of ^{229}Th as observed in the α decay of ^{233}U. Nucl. Phys. A **259**, 29–60 (1976). https://doi.org/10.1016/0375-9474(76)90494-2
10. Y.A. Akavoli, Nuclear data sheets for $A = 229$. Nucl. Data Sheets **58**, 555–588 (1989). https://doi.org/10.1016/0090-3752(89)80025-0
11. C.W. Reich, R.G. Helmer, *Proceedings of the International Symposium on Nuclear Physics of Our Times* (World Scientific, Singapore, 1993), p. 474. https://doi.org/10.1142/1989
12. T. Sikorsky, J. Geist, D. Hengstler et al., Measurement of ^{229}Th isomer energy with a magnetic microcalorimeter. Phys. Rev. Lett. **125**, 142503 (2020). https://doi.org/10.1103/PhysRevLett.125.142503
13. P.V. Bilous, H. Bekker, J. Berengut et al., Electronic bridge excitation in highly charged Th-229 ions. Phys. Rev. Lett. **124**, 192502 (2020). https://doi.org/10.1103/PhysRevLett.124.192502
14. S.G. Porsev, V.V. Flambaum, E. Peik et al., excitation of the isomeric ^{229m} Th nuclear state via an electronic bridge process in $^{229}Th^{+}$. Phys. Rev. Lett. **105**, 182501 (2010). https://doi.org/10.1103/PhysRevLett.105.182501
15. B.A. Zon, F.F. Karpeshin, Acceleration of the decay of 235mU by laser-induced resonant internal conversion. Sov. Phys. JETP **70**, 224–227 (1990)
16. L. von der Wense, P.V. Bilous, B. Seiferle et al., The theory of direct laser excitation of nuclear transitions. Eur. Phys. J. A **56**, 176 (2020). https://doi.org/10.1140/epja/s10050-020-00177-x
17. B. Seiferle, L. von der Wense, P.V. Bilous et al., Energy of the ^{229}Th nuclear clock transition. Nature **573**, 243–246 (2019). https://doi.org/10.1038/s41586-019-1533-4
18. J.M. Blatt, V.F. Weisskopf, *Theoretical Nuclear Physics* (Wiley, New York, 1952). https://doi.org/10.1007/978-1-4612-9959-2
19. N. Minkov, A. Pálffy, Theoretical predictions for the magnetic dipole moment of ^{229m}Th. Phys. Rev. Lett. **122**, 162502 (2019). https://doi.org/10.1103/PhysRevLett.122.162502
20. J. Blaise, J. Wyart, Selected constants: energy levels and atomic spectra of actinides. http://www.lac.u-psud.fr/Database/Contents.htmlhttp://www.lac.u-psud.fr/Database/Contents.html
21. U.I. Safronova, W.R. Johnson, M.S. Safronova, Excitation energies, polarizabilities, multipole transition rates, and lifetimes in Th IV. Phys. Rev. A **74**, 042511 (2006). https://doi.org/10.1103/PhysRevA.74.042511
22. M.S. Safronova, U.I. Safronova, Relativistic many-body calculation of energies, oscillator strengths, transition rates, lifetimes, polarizabilities, and quadrupole moment of a Fr-like Th IV ion. Phys. Rev. A **87**, 062509 (2013). https://doi.org/10.1103/PhysRevA.87.062509
23. B.W. Shore, K. Bergmann, A. Kuhn et al., Phys. Rev. A **45**(7), 5297–5300 (1992). https://doi.org/10.1103/PhysRevA.45.5297
24. B.W. Shore, Picturing stimulated Raman adiabatic passage: a STIRAP tutorial. Adv. Opt. Photon. **9**, 563–719 (2017). https://doi.org/10.1364/AOP.9.000563
25. F.F. Karpeshin, I.M. Band, M.B. Trzhaskowskaya et al., Study of 229Th through laser-induced resonance internal conversion. Phys. Lett. B **282**, 267–270 (1992). https://doi.org/10.1016/0370-2693(92)90636-I
26. S.G. Porsev, V.V. Flambaum, Effect of atomic electrons on the 7.6-eV nuclear transition in $^{229}Th^{3+}$. Phys. Rev. A **81**, 032504 (2010). https://doi.org/10.1103/81.032504